ACS Macro Letters

Letter

pubs.acs.org/macroletters

Structural Characteristics of Amphiphilic Cyclic and Linear Block Copolymer Micelles in Aqueous Solutions

Kyuyoung Heo,[†,∥] Young Yong Kim,[†,∥] Yu Kitazawa,[‡,∥] Mihee Kim,[†] Kyeong Sik Jin,[§] Takuya Yamamoto,*[,‡] and Moonhor Ree*[,†]

[†]Department of Chemistry, Division of Advanced Materials Science, Center for Electro-Photo Behaviors in Advanced Molecular Systems, Pohang Accelerator Laboratory, Polymer Research Institute, and BK School of Molecular Science, Pohang University of Science & Technology, Pohang 790-784, Republic of Korea

[‡]Department of Organic and Polymeric Materials, Tokyo Institute of Technology, O-okayama, Meguro-ku, Tokyo 152-8552, Japan

[§]Pohang Accelerator Laboratory, Pohang University of Science & Technology, Pohang 790-784, Republic of Korea

Supporting Information

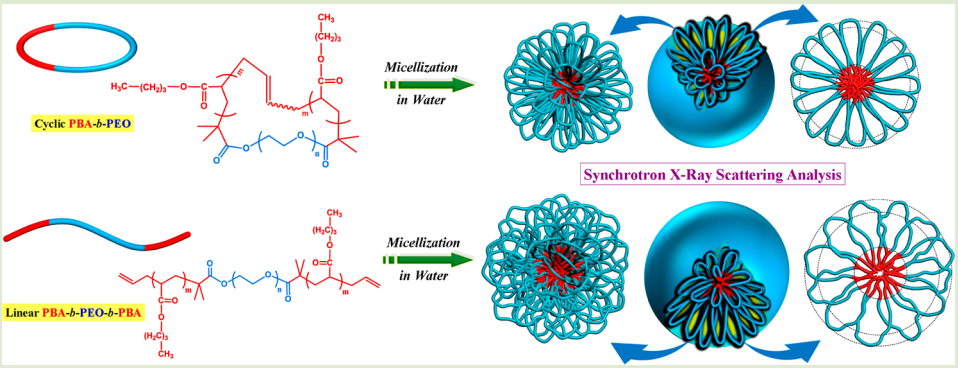

ABSTRACT: The structural characteristics of aqueous micelles composed of amphiphilic cyclic poly(*n*-butyl acrylate-*b*-ethylene oxide) (cyclic PBA-*b*-PEO) or a linear analogue (i.e., linear poly(*n*-butyl acrylate-*b*-ethylene oxide-*b*-*n*-butyl acrylate) (linear PBA-*b*-PEO-*b*-PBA)) were examined for the first time using synchrotron X-ray scattering techniques and quantitative data analysis. The scattering data were analyzed using a variety of methodologies in a comprehensive complementary manner. These analyses provided details of the structural information about the micelles. Both micelles were found to consist of a core and a fuzzy shell; however, the cyclic block copolymer had a strong tendency to form micelles with core and shell parts that were more compact and dense than the corresponding parts of the linear block copolymer micelles. The PBA block of the cyclic copolymer was found to form a hydrophobic core with a density that exceeded the density of the homopolymer in the bulk state. The structural differences originated primarily from the topological difference between the cyclic and linear block copolymers. The elimination of the chain end groups (which introduced entropy and increased the excess excluded volume) from the amphiphilic block copolymer yielded more stable dense micelles in solution.

The chain architectures of block copolymers can influence their self-assembly characteristics in both aqueous and organic solvents.[1−8] Amphiphilic block copolymers commonly form micelles in solvents that are selective for one of the blocks, thereby promoting the formation of core−shell micelle structures composed of a relatively compact micellar core surrounded by a soluble corona or shell layer.[1−3] Linear diblock copolymers tend to form star-like micellar structures,[4] whereas linear triblock copolymers tend to form flower-like micelles in which the two end blocks fold back into the core and form loops above a critical micelle concentration (CMC) via an entropy-driven closed association mechanism.[5−7] Recently, several new synthetic methodologies were introduced for the preparation of cyclic homopolymers and block copolymers.[1,3,6−9] Some of the cyclic block copolymers were investigated in aspects of micelle formation characteristics.[10−12]

Certain amphiphilic cyclic block copolymer systems formed micelles with significantly higher salt and thermal stabilities compared to the corresponding linear block copolymers.[7] The structural properties of these cyclic block copolymer micelles have not yet been explored in detail.

In this study, we investigated the structural properties of micelles formed in water by a cyclic poly(*n*-butyl acrylate-*b*-ethylene oxide) (PBA-*b*-PEO) and its linear poly(*n*-butyl acrylate-*b*-ethylene oxide-*b*-*n*-butyl acrylate) (PBA-*b*-PEO-*b*-PBA) analogue using synchrotron X-ray scattering techniques. A cyclic PBA-*b*-PEO polymer and its linear PBA-*b*-PEO-*b*-PBA analogue (Figure 1) were prepared according to the synthetic

Received: January 13, 2014
Accepted: February 17, 2014
Published: February 18, 2014

   dx.doi.org/10.1021/mz5000224 | *ACS Macro Lett.* 2014, 3, 233−239

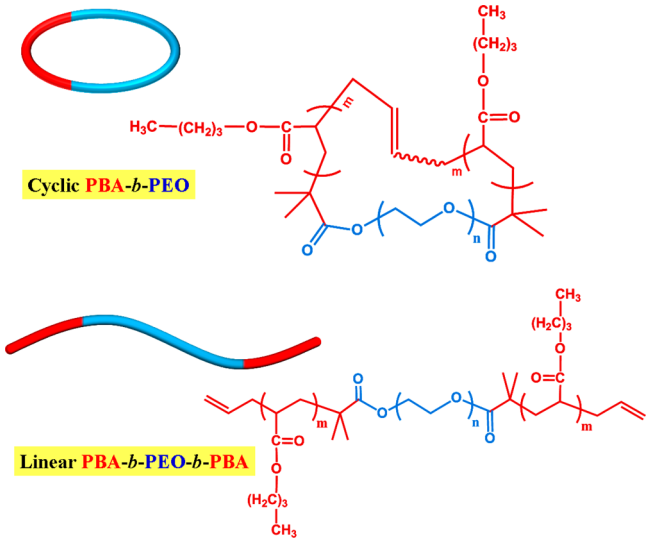

Figure 1. Chemical structures of cyclic and linear block copolymers.

schemes reported previously.[6,7] The syntheses are described in detail in the Supporting Information. The linear triblock copolymer was characterized to have a composition of $[H_2C{=}CHCH_2(BA)_{5.1}C(CH_3)_2]{-}[COO(EO)_{69.0}CO]{-}[C(CH_3)_2(BA)_{5.1}CH_2CH{=}CH_2]$ and a molecular weight $M_{n,NMR}$ of [740]−[3110]−[740] by proton nuclear magnetic resonance (^{1}H NMR) spectroscopy (Figure S1 in the Supporting Information); here, the nonpolar or less polar (i.e., hydrophobic) parts of the linkers were included into the $M_{n,NMR}$ of the hydrophobic PBA blocks, whereas the polar (i.e., hydrophilic) parts of the linkers were included into the $M_{n,NMR}$ of the hydrophilic PEO block. From the $M_{n,NMR}$ values of the blocks and the mass densities of PBA and PEO homopolymers (d_{PBA} = 1.08 g/cm^3 and d_{PEO} = 1.12 g/cm^3), the volume ratio of the PBA and PEO blocks in the linear block copolymer was estimated to be 0.331/0.669. The linear block copolymer was further determined to have an overall number-average molecular weight $\overline{M}_n$ of 5850 and a polydispersity index (PDI) of 1.11 by the gel permeation chromatography (GPC) analysis calibrated with polystyrene standards (Figure S2, Supporting Information). The cyclic block copolymer was determined to have a composition of $[C(CH_3)_2(BA)_{5.3}H_2CCH{=}CHCH_2(BA)_{5.3}C(CH_3)_2]{-}[COO(EO)_{67.7}CO]$ and a molecular weight $M_{n,NMR}$ of [1500]−[3050] (Figure S3, Supporting Information). From the $M_{n,NMR}$, d_{PBA}, and d_{PEO} values, the volume ratio of the PBA and PEO blocks in the cyclic block copolymer was obtained to be 0.334/0.666. The cyclic block copolymer was measured to have $\overline{M}_n$ = 4700 and PDI = 1.18 by GPC analysis (Figure S4, Supporting Information).

Aqueous micellar solutions were prepared from the linear and cyclic block copolymers as described previously.[7] Each block copolymer was dissolved in tetrahydrofuran (THF) to prepare 2 mL of a 10 mg/mL solution. Deionized distilled water was added in a dropwise manner at a rate of one drop per 5 s to the polymer solution with vigorous stirring. THF was removed from the resulting solution using a rotary evaporator. The resulting micellar solution was filtered using a disposable syringe equipped with a cellulose acetate filter with a pore size of 0.2 μm. In this manner, a series of aqueous micellar solutions were prepared with concentrations that ranged from 1.0 to 5.0 mg/mL. These micellar solutions were checked using dynamic light scattering (DLS) before X-ray scattering analysis. The DLS analysis confirmed that the micelles formed in the individual solutions revealed a unimodal size distribution (Figure S5, Supporting Information). The micellar solutions were submitted to synchrotron X-ray scattering measurements carried out at the 4C beamline[13] of the Pohang Light Source in POSTECH (Supporting Information). These measurements revealed that both the linear and cyclic block copolymer 5.0 mg/mL solutions gave high-quality scattering data with negligible contributions from the structure factors of the micelles.

Representative X-ray scattering data are presented in Figure 2. The scattering data were analyzed by considering several

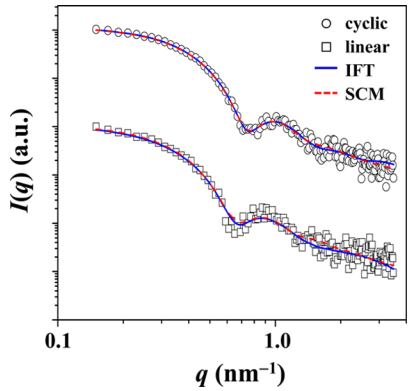

Figure 2. X-ray scattering profiles of the micelles formed in water, which were measured at room temperature: (○) cyclic PBA-*b*-PEO micelle; (□) linear PBA-*b*-PEO-*b*-PBA micelle. The black symbols are the measured data; the blue solid and red dashed lines were obtained by fitting the data using the IFT method and SCM models, respectively.

possible structural models using a variety of methodologies. Several analytical schemes, including Guinier analysis,[14,15] the indirect Fourier transform (IFT) method,[15,16] Kratky analysis,[17] spherical copolymer micelle (SCM) model analysis,[18] and core−fuzzy shell (CFS) model analysis,[15,19,20] were found to be the most suitable. Derivations of these analytical schemes are provided in the Supporting Information.

The measured scattering data were first analyzed using the Guinier approach, which provided information about the micelle sizes formed in the block copolymer solutions. This analysis revealed that the radius of gyration $R_{g,G}$ was 5.62 nm for the linear block copolymer micelles and 5.16 nm for the cyclic block copolymer micelles (Table 1 and Figure S6, Supporting Information).

The X-ray scattering data were further analyzed in detail using the IFT method, which extracted structural information directly from the scattering data using numerical methods without building a specific parametrized model. This approach minimized the impact of the missing data, providing the pair distance distribution function $p(r)$ and the relative radial electron density distribution function $\Delta\rho(r)$, where r is the distance between the paired scattering elements in the micelle. The scattering data were satisfactorily analyzed using the IFT method. The analysis results are presented in Figure 3 and Table 1. The $p(r)$ profiles revealed a bell-like shape, indicating that the micelles that had formed in the linear and cyclic block copolymer solutions were in globular (i.e., spherical) shapes (Figure 3a). The globular micelles formed in the linear

dx.doi.org/10.1021/mz5000224 | ACS Macro Lett. 2014, 3, 233−239

Table 1. Structural Parameters of Micelles of the Linear and Cyclic Block Copolymers Obtained from Analysis of the Measured X-ray Scattering Data

structural parameter	linear block copolymer	cyclic block copolymer
Guinier analysis		
$R_{g,G}$[a] (nm)	5.62 (0.02)[n]	5.16 (0.01)[n]
IFT analysis		
$R_{g,IFT}$[a] (nm)	5.10	4.85
D_{max}[b] (nm)	13.0	12.5
r_{max}[c] (nm)	6.72	6.44
$r_{c,IFT}$[d] (nm)	1.94	1.78
SCM analysis		
r_{SCM}[e] (nm)	6.47 (0.03)	5.83 (0.02)
$r_{c,SCM}$[d] (nm)	1.85 (0.01)	1.70 (0.01)
$t_{s,SCM}$[f] (nm)	4.62 (0.03)	4.13 (0.02)
$R_{g(PEO),SCM}$[g] (nm)	2.18 (0.01)	1.93 (0.01)
d[h]	1.12 (0.01)	1.14 (0.01)
N_{agg}[i]	11.61 (0.01)	10.02 (0.01)
$r_{c,theory}$[j] (nm)	1.92 (0.01)	1.86 (0.01)
CFS analysis		
r_{CFS}[e] (nm)	6.50 (0.02)	5.96 (0.01)
$r_{c,CFS}$[d] (nm)	1.85 (0.17)	1.69 (0.15)
$t_{s,CFS}$[f] (nm)	4.65 (0.17)	4.27 (0.15)
$\sigma_{f,CFS}$[k] (nm)	0.89 (0.05)	0.64 (0.03)
$\sigma_{f,CFS}/t_{s,CFS}$[l] (%)	19.1 (1.3)	15.0 (0.8)
$\bar{\xi}$[m] (nm)	1.71 (0.09)	1.23 (0.07)

[a]Radius of gyration of micelle. [b]Maximum dimension (i.e., diameter) of micelle determined from the $p(r)$ profile. [c]Radius of micelle determined from the peak maximum of the $p(r)$ profile. [d]Radius of core. [e]Radius of micelle. [f]Thickness of shell; in the case of corona type shell, the shell thickness was calculated from a formula, $t_{s,SCM} = (1 + d) R_{g(PEO),SCM}$. [g]Radius of gyration of the PEO block chains in the shell part. [h]Degree of penetration of corona chain to core; $d \cong 1$ for mimicking nonpenetration of the corona chains. [i]Aggregation number of copolymer chains in the micelle. [j]Theoretical radius of core calculated from the determined N_{agg} value and the mass density of PBA. [k]Thickness of the fuzzy part in shell. [l]Fuzziness. [m]Average correlation length of density fluctuation. [n]Error bar extracted over the sweep range ±1.0% of the χ^2 term obtained by best-fitting the X-ray scattering data with a most proper structural model; here the χ^2 term is the sum of the squared deviations between the experimental X-ray scattering data and the fitted profile.

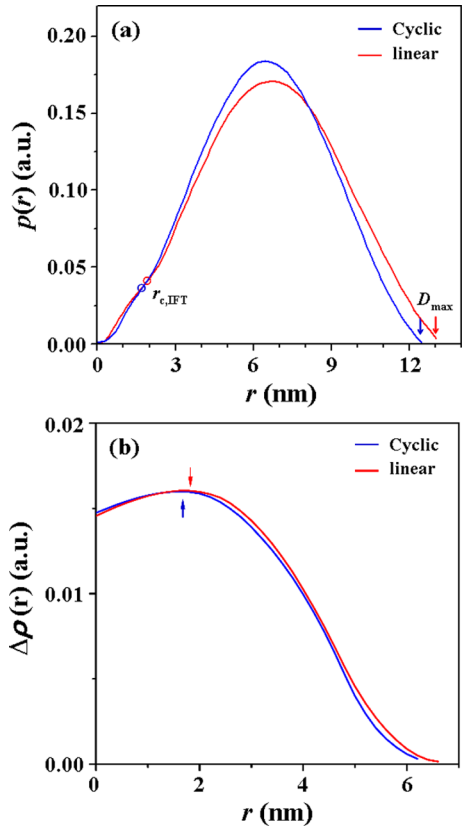

Figure 3. (a) Pair distance distribution functions $p(r)$ and (b) density distribution functions $\rho(r)$ obtained by the IFT analysis of the X-ray scattering data in Figure 2: (blue line) cyclic PBA-*b*-PEO micelle; (red line) linear PBA-*b*-PEO-*b*-PBA micelle.

copolymer solution had a radius of gyration $R_{g,IFT}$ of 5.10 nm, with a peak maximum occurring at r = 6.72 nm (= r_{max}, corresponding to the micelle radius). These values yielded a maximum diameter D_{max} of 13.00 nm. By contrast, the globular micelles formed in the cyclic copolymer solution were characterized by an $R_{g,IFT}$ = 4.85 nm, r_{max} = 6.44 nm, and D_{max} = 12.50 nm. It should be noted that the $R_{g,IFT}$ values were slightly smaller than the $R_{g,G}$ values reported above. These $R_{g,IFT}$ and $R_{g,G}$ results confirmed that the cyclic block copolymer formed micelles that were slightly smaller than those formed by the corresponding linear block copolymer.

The $p(r)$ profiles revealed an inflection point in the low r region (Figure 3a), indicating that the internal electron density displayed a distinct change at a specific r value. This type of feature is consistent with the formation of an interface between two different phases, suggesting that the micelles were composed of a core and a shell. The inflection point of the r value was, therefore, assigned as the radius of the core part of the micelle, $r_{c,IFT}$. The $r_{c,IFT}$ values were determined to be 1.94 nm for the micelles formed by the linear block copolymer and 1.78 nm for the micelles formed by the cyclic block copolymer.

An ideally homogeneous micelle (i.e., a sphere) would be expected to display a $p(r)$ profile with a maximum peak at r = 1.36$R_{g,IFT}$ (i.e., $r/R_{g,IFT}$ = 1.36). Here, the $p(r)$ profile displayed a maximum at $r/R_{g,IFT}$ = 1.28 for the micelles formed by the linear copolymer and a maximum at $r/R_{g,IFT}$ = 1.26 for the micelles formed by the cyclic copolymer. The observation of a core−shell micelle structure suggested that the core and shell phases were inhomogeneous, rather than homogeneous, in their density distribution. The $p(r)$ profiles were slightly asymmetric and displayed a weak small tail in the high-r region. The asymmetric characteristics, with a relatively low $r_{max}/R_{g,IFT}$ value, suggested that the surfaces of the micelles were fuzzy due to fluctuations in the density distribution.[19] The inhomogeneities in the density distribution were observed in the relative radial density distribution function $\Delta\rho(r)$ profiles, as shown Figure 3b. The cyclic block copolymer micelle yielded a $\Delta\rho(r)$ profile with a maximum at r = 1.78 nm (blue arrow, Figure 3b), which corresponded to the core radius $r_{c,IFT}$ determined from the inflection point of the $p(r)$ profile. The linear block copolymer micelle yielded a $\Delta\rho(r)$ profile with a maximum at r = 1.94 nm (red arrow, Figure 3b), which corresponded to the $r_{c,IFT}$ value. The electron density ρ_e of each polymer is known: 355 nm^{-3} for PBA polymers ($\rho_{e,PBA}$), 367 nm^{-3} for PEO polymers ($\rho_{e,PEO}$), and 334 nm^{-3} for water ($\rho_{e,water}$). These ρ_e values were combined with the maxima obtained from the $\Delta\rho(r)$ profiles and the inflection points in the $p(r)$ profiles to model the micelles as consisting of two phases with different

dx.doi.org/10.1021/mz5000224 | ACS Macro Lett. 2014, 3, 233−239

electron densities. PEO polymers are hydrophilic, whereas PBA polymers are hydrophobic. Therefore, the shell part in contact with water was assigned as the PEO block chains, whereas the core was assigned as the hydrophobic PBA block chains, which were more stable when separated from the water interface.

The above results were considered in a further analysis of the measured X-ray scattering data using SCM models comprising a dense core and a swollen corona. As shown in Figure 2, the X-ray scattering data could be satisfactorily fit using an SCM model. The fit results are summarized in Table 1. The core radius $r_{c,SCM}$ was 1.85 nm for the micelles composed of the linear block copolymer and 1.70 nm for those composed of the cyclic block copolymer. These $r_{c,SCM}$ values were slightly shorter than those ($r_{c,IFT}$ = 1.94 and 1.78 nm) estimated using the IFT analysis of the scattering data. The aggregation number N_{agg} of the block copolymer chains in the micelle was determined to be 11.61 for the micelle composed of the linear block copolymer having two end PBA blocks ($M_{n,NMR}$ = 740) or 10.02 for the micelle composed of the cyclic block copolymer having only one PBA block ($M_{n,NMR}$ = 1500).

The structural characteristics of the corona (i.e., shell) parts were also obtained from the SCM analysis (Table 1). The corona thickness values, $t_{s,SCM}$, were 4.62 nm for the linear block copolymer micelle and 4.13 nm for the cyclic block copolymer micelle. The hydrophilic PEO block in the corona part was determined to have a radius of gyration $R_{g(PEO),SCM}$ of 2.18 nm for the linear block copolymer micelle and 1.93 nm for the cyclic block copolymer micelle. The $t_{s,SCM}$ values for both block copolymer micelles were slightly larger than twice the $R_{g(PEO),SCM}$ values. These results determined two important structural characteristics as follows. The PEO blocks in the corona region assumed fairly extended chain conformations, possibly due to the swelling of the block chains, which maximized the number of block chain−solvent contacts. The PEO block chains in the corona region did not penetrate the core part of the micelle.

The fuzzy surface characteristics of the micelles (as observed in the IFT analysis above) were evident from the Kratky analysis of the scattering data. As shown in Figure 4a, the X-ray scattering profiles of both the linear copolymer and the cyclic copolymer revealed a q^{-2} dependency in the intermediate q region, indicating that the PEO block chains of the shell part in contact with water (a good solvent for the PEO blocks) were flexible, similar to a Gaussian coil. Furthermore, the scattering profiles exhibited a $q^{-5/3}$ dependency in the high-q region (q > 1.8 nm^{-1}), further indicating the absence of a sharp interface between the shell part and the water solvent medium. The interface between the micelle shell and the water medium was fuzzy.

The X-ray scattering data were further analyzed using CFS models. As shown in Figure 4b and c, the scattering data could be satisfactorily fitted using CFS models comprising blob contributions. The obtained structural parameters are summarized in Table 1. The core radius $r_{c,CFS}$ was 1.85 nm for the linear block copolymer micelle and 1.69 nm for the cyclic block copolymer micelle, and these values were reasonably consistent with those obtained from the SCM analysis. The fuzzy shell thickness values, $t_{s,CFS}$, were 4.65 nm for the linear block copolymer micelle and 4.27 nm for the cyclic block copolymer micelle and were slightly larger than the corona shell thicknesses $t_{s,SCM}$ obtained from the SCM analysis. The thickness values of the fuzzy parts, $\sigma_{f,CFS}$, were 0.89 nm for the linear block copolymer micelle and 0.64 nm for the cyclic

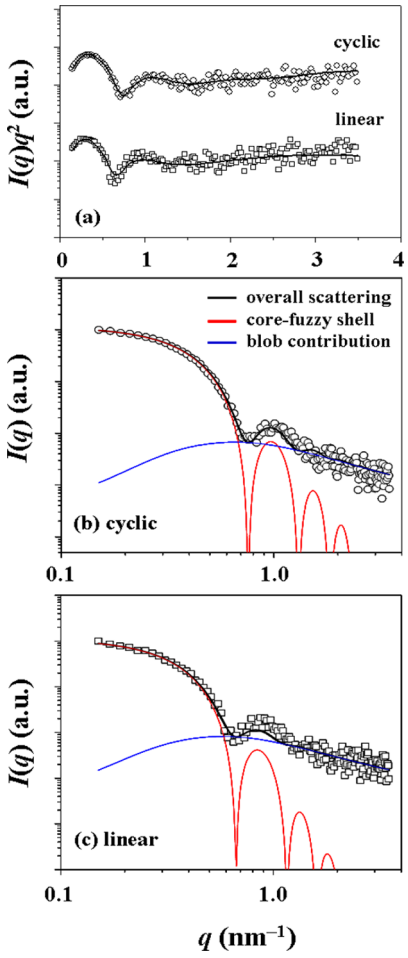

Figure 4. X-ray scattering profiles of the cyclic PBA-*b*-PEO and linear PBA-*b*-PEO-*b*-PBA micelles formed in water, which were measured at room temperature: (a) Kratky representations where the black symbols are the measured data and the solid lines represent the profiles obtained by fitting the data using SCM models; (b,c) X-ray scattering profiles in which the black symbols are the measured data and the black solid lines represent the sum of the profiles obtained by fitting the data using CFS models (red lines) and blob contributions (blue lines).

block copolymer micelle. The $t_{s,SCM}$ and $\sigma_{f,CFS}$ values yielded fuzziness values (= $\sigma_{f,CFS}/t_{s,SCM}$) for the fuzzy shells of 19.1% for the linear block copolymer micelle and 15.0% for the cyclic block copolymer micelle. On the other hand, the average correlation length of the density fluctuation $\bar{\xi}$ in the fuzzy shell part was found to be 1.71 nm for the linear block copolymer micelle and 1.23 nm for the cyclic block copolymer micelle.

The above determined N_{agg} and r_c values permitted estimation of the core density in a micelle. As listed in Table 1, the r_c value of the micelle was determined to vary a little bit depending on the scattering data analysis methods: the r_c value was 1.85−1.94 nm for the linear copolymer micelle and 1.69−1.78 nm for the cyclic copolymer micelle. These r_c values were directly reflected into the core density estimation. The core density d_{core} was 0.93−1.08 g/cm^3 for the linear copolymer micelle and 1.06−1.23 g/cm^3 for the cyclic copolymer micelle. The d_{core} value of the cyclic copolymer micelle is always larger than that of the linear copolymer micelle (which is slightly less than or the same as the density (d = 1.08 g/cm^3) of linear PBA homopolymer in the bulk solid state). Surprisingly, the cyclic

dx.doi.org/10.1021/mz5000224 | *ACS Macro Lett.* 2014, 3, 233−239

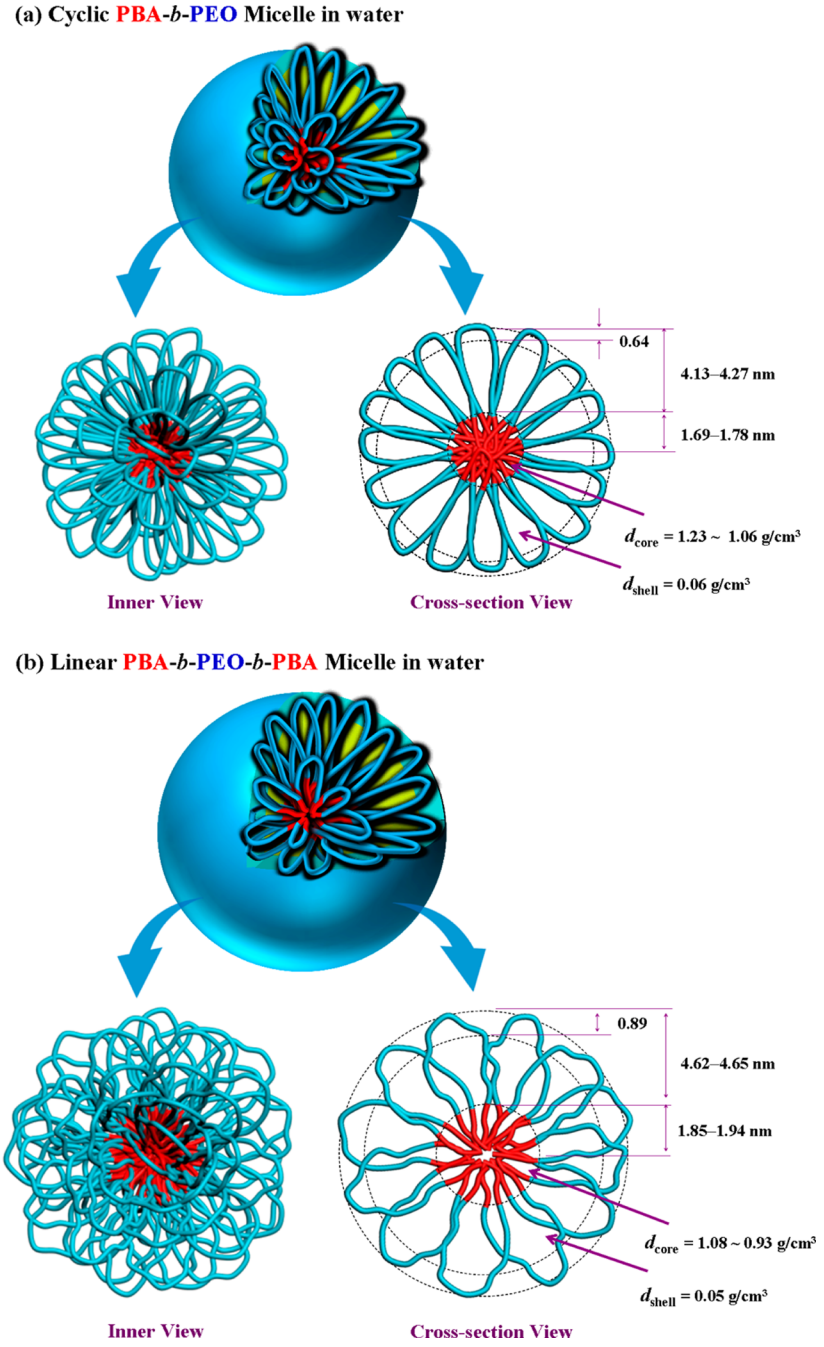

Figure 5. Schematic representations of the phase-separated nanostructures for (a) cyclic PBA-*b*-PEO-*b*-PBA and (b) linear PBA-*b*-PEO micelles formed in water; the structural parameters were obtained by the analyses of the X-ray scattering data using the Guinier method, IFT method, SCM models, and CFS models.

copolymer micelle d_{core} is further very close to or larger than that of the linear PBA homopolymer in the bulk solid state. However, cyclic polymers are generally known to reveal relatively higher densities than those of the corresponding linear polymers in the literature.[21] Taking this fact into account, the d_{core} of the cyclic copolymer micelle is expected to be comparable to that of the cyclic PBA homopolymer in the bulk solid state (which can be larger than that of the corresponding linear polymer).

The N_{agg} values together with the hydrophobic PBA block molecular weights further permitted estimation of the theoretical radii of the core $r_{c,theory}$ using the mass density of the PBA homopolymer under the assumption that the micellar core was close-packed (see the derivation described in the Supporting Information). The estimated $r_{c,theory}$ was 1.92 nm for the linear block copolymer micelle core and 1.86 nm for the cyclic block copolymer micelle core. The $r_{c,theory}$ value of the linear copolymer micelle was slightly larger than the $r_{c,SCM}$ and $r_{c,CFS}$ values but very slightly smaller than the $r_{c,IFT}$ value (Table 1). In contrast, the $r_{c,theory}$ value of the cyclic copolymer micelle was always smaller than the $r_{c,SCM}$, $r_{c,CFS}$, and $r_{c,IFT}$ values (Table 1).

These d_{core} and $r_{c,theory}$ results collectively confirmed that during micelle formation the cyclic block copolymer formed a denser core than the corresponding linear block copolymer. Moreover, the PBA block chains in the core of the cyclic

dx.doi.org/10.1021/mz5000224 | *ACS Macro Lett.* 2014, 3, 233−239

copolymer micelle were packed more densely than the PBA homopolymer packing density in the bulk state at room temperature. The observation of such the dense PBA core in the cyclic copolymer micelle indicated that the PBA block chains were well packed in a relatively extended chain conformation rather than in a random coil conformation. The formation of a dense core by the cyclic block copolymer may have been attributed to the favorable intra- and interchain interactions of the PBA blocks, which were free from disruptions in the polymer chain packing because the open-chain terminal groups had a relatively high entropy and an excess excluded volume.

In addition, the t_s and N_{agg} values permitted the PEO block chain densities in the corona regions to be estimated, yielding values of 0.05 g/cm^3 for the linear block copolymer micelle and 0.06 g/cm^3 for the cyclic block copolymer micelle. These results collectively indicated that the shell of the cyclic block copolymer micelle was thinner but denser than that of the linear block copolymer micelle. These qualities were mainly attributed to the formation of a smaller denser core, which provided a surface to which the PEO block chains could anchor.

The results discussed above were used to construct phase-separated structural models of the aqueous micelles composed of linear or cyclic block copolymers, as shown in Figure 5.

In summary, the synchrotron X-ray scattering measurements and data analysis revealed that both the linear PBA-*b*-PEO-*b*-PBA and the cyclic PBA-*b*-PEO polymers formed stable micelles in an aqueous solution. The structural parameters of the micelles were determined for the first time through a quantitative analysis of the X-ray scattering data involving several appropriate and complementary methods. Both micelles were found to be composed of a core part and a fuzzy shell part. The cores and shells formed a relatively sharp interface. The cyclic block copolymer micelle formed a more compact and denser hydrophobic PBA block chain core, compared to the density of the core formed by linear block copolymer micelle. The cyclic block copolymer micelle formed a thinner and denser hydrophilic PEO block chain shell with a shallower fuzzy surface layer. Interestingly, the PBA core and PEO shell parts of the cyclic block copolymer micelle were more extended than the corresponding chains in the linear block copolymer micelle. The structural differences originated primarily from the topological differences resulting from the properties of the chemical structures. The presence of two free terminal groups in the linear block copolymer penalized the micelle formation in solution by increasing the size and decreasing the packing density of the core and shell parts by increasing the entropy and the excluded volume. Eliminating the end groups from the amphiphilic block copolymer appeared to promote the creation of more stable dense micelles in solution.

■ ASSOCIATED CONTENT

Supporting Information

Synthesis of linear and cyclic block copolymers, synchrotron X-ray scattering measurements, X-ray scattering data analyses, NMR spectra, GPC data, DLS data, and Guinier plots. This material is available free of charge via the Internet at http://pubs.acs.org.

■ AUTHOR INFORMATION

Corresponding Authors

*Tel.: +82-54-279-2120. Fax: +82-54-279-3399. E-mail: ree@postech.edu (M.R.).

*Tel.: +81-3-5734-2438. Fax: +81-3-5734-2876. E-mail: yamamoto.t.ay@m.titech.ac.jp (T.Y.).

Author Contributions

‖Authors K.H., Y.Y.K., and Y.K. contributed equally to this work.

Notes

The authors declare no competing financial interest.

■ ACKNOWLEDGMENTS

This study was supported by the National Research Foundation (NRF) of Korea (Doyak Program 2011-0028678 and Center for Electro-Photo Behaviors in Advanced Molecular Systems (2010-0001784)) and the Ministry of Science, ICT & Future Planning (MSIP), and the Ministry of Education (BK21 Plus Program and Global Excel Program). This study was also supported by Yazaki Memorial Foundation for Science and Technology and KAKENHI (23685022 and 23106709). The synchrotron X-ray scattering measurements at the Pohang Accelerator Laboratory were supported by MSIP, POSTECH Foundation, and POSCO Company. We thank Dr. Satoshi Honda and Prof. Yasuyuki Tezuka for their assistance on the synthesis of the block copolymers.

■ REFERENCES

(1) Riess, G. *Prog. Polym. Sci.* **2003**, *28*, 1107−1170.

(2) (a) Alexandridis, P.; Lindman, B. *Amphiphilic Block Copolymers: Self-Assembly and Applications*; Elsevier: Amsterdam, 2000. (b) Chu, B. *Langmuir* **1995**, *11*, 414−421.

(3) Booth, C.; Attwood, D. *Macromol. Rapid Commun.* **2000**, *21*, 501−527.

(4) (a) Kim, Y. H.; Ford, W. T.; Mourey, T. H. *J. Polym. Sci., Part A: Polym. Chem. Ed.* **2007**, *45*, 4623−4634. (b) Pang, X. C.; Zhao, L.; Akinc, M.; Kim, J. K.; Lin, Z. Q. *Macromolecules* **2011**, *44*, 3746−3752.

(5) (a) Alexandridis, P.; Lindman, B. *Amphiphilic Block Copolymers: Self Assembly and Applications*; Elsevier: Amsterdam, 2000. (b) Balsara, N. P.; Tirrell, M.; Lodge, T. P. *Macromolecules* **1991**, *24*, 1975−1986. (c) Zhou, Z. K.; Chu, B.; Peiffer, D. G. *Langmuir* **1995**, *11*, 1956−1965.

(6) Adachi, K.; Honda, S.; Hayashi, S.; Tezuka, Y. *Macromolecules* **2008**, *41*, 7898−7903.

(7) (a) Honda, S.; Yamamoto, T.; Tezuka, Y. *J. Am. Chem. Soc.* **2010**, *132*, 10251−10253. (b) Honda, S.; Yamamoto, T.; Tezuka, Y. *Nat. Commun.* **2013**, *4*, 1574.

(8) (a) Sugai, N.; Heguri, H.; Ohta, K.; Meng, Q.; Yamamoto, T.; Tezuka, Y. *J. Am. Chem. Soc.* **2010**, *132*, 14790−14802. (b) Sugai, N.; Heguri, H.; Yamamoto, T.; Tezuka, Y. *J. Am. Chem. Soc.* **2011**, *133*, 19694−19697. (c) Hatakeyama, F.; Yamamoto, T.; Tezuka, Y. *ACS Macro Lett.* **2013**, *2*, 427−431.

(9) (a) Baba, E.; Honda, S.; Yamamoto, T.; Tezuka, Y. *Polym. Chem.* **2011**, *3*, 1903−1909. (b) Stamenovic, M. M.; Espeel, P.; Baba, E.; Yamamoto, T.; Tezuka, Y.; Du Prez, F. E. *Polym. Chem.* **2013**, *4*, 184−193. (c) Zhang, B.; Zhang, H.; Li, Y.; Hoskins, J. N.; Grayson, S. M. *ACS Macro Lett.* **2013**, *2*, 845−848. (d) Poelma, J. E.; Ono, K.; Miyajima, D.; Aida, T.; Satoh, K.; Hawker, C. J. *ACS Nano* **2012**, *6*, 10845−10854.

(10) Iatrou, H.; Hadjichristidis, N.; Meier, G.; Frielinghaus, H.; Monkenbusch, M. *Macromolecules* **2002**, *35*, 5426−5437.

(11) (a) Di Cola, E.; Lefebvre, C.; Deffieux, A.; Narayanan, T.; Borsali, R. *Soft Matter* **2009**, *5*, 1081−1090. (b) Minatti, E.; Borsali, R.; Schappacher, M.; Deffieux, A.; Soldi, V.; Narayanan, T.; Putaux, J.-L. *Macromol. Rapid Commun.* **2002**, *23*, 978−982. (c) Minatti, E.; Viville,

P.; Borsali, R.; Schappacher, M.; Deffieux, A.; Lazzaroni, R. *Macromolecules* **2003**, *36*, 4125−4133. (d) Yu, G.-E.; Garrett, C. A.; Mai, S.-M.; Altinok, H.; Attwood, D.; Price, C.; Booth, C. *Langmuir* **1998**, *14*, 2278−2285.
(12) (a) Zhulina, E. B.; Borisov, O. V. *ACS Macro Lett.* **2013**, *2*, 292−295. (b) Kim, K. H.; Huh, J.; Jo, W. H. *J. Chem. Phys.* **2003**, *118*, 8468−8475.
(13) (a) Yoon, J.; Kim, K.-W.; Kim, J.; Heo, K.; Jin, K. S.; Jin, S.; Shin, T. S.; Lee, B.; Rho, Y.; Ahn, B.; Ree, M. *Macromol. Res.* **2008**, *16*, 575−585. (b) Kim, M.; Rho, Y.; Jin, K. S.; Ahn, B.; Jung, S.; Kim, H.; Ree, M. *Biomacromolecules* **2011**, *12*, 1629−1640. (c) Jin, K. S.; Shin, S. R.; Ahn, B.; Jin, S.; Rho, Y.; Kim, H.; Kim, S. J.; Ree, M. *J. Phys. Chem. B* **2010**, *114*, 4783−4788. (d) Shin, S. R.; Jin, K. S.; Lee, C. K.; Kim, S. I.; Spinks, G. M.; So, I.; Jeon, J.-H.; Kang, T. M.; Mun, J. Y.; Han, S.-S.; Ree, M.; Kim, S. J. *Adv. Mater.* **2009**, *21*, 1907−1910.
(14) Guinier, A.; Fournet, G. *Small Angle Scattering X-Ray*; Wiley: New York, 1955.
(15) (a) Jin, S.; Higashihara, T.; Jin, K. S.; Yoon, J.; Rho, Y.; Ahn, B.; Kim, J.; Hirao, A.; Ree, M. *J. Phys. Chem. B* **2010**, *114*, 6247−6257. (b) Jin, S.; Jin, K. S.; Yoon, J.; Heo, K.; Kim, J.; Kim, K.-W.; Ree, M.; Higashihara, T.; Watanabe, T.; Hirao, A. *Macromol. Res.* **2008**, *16*, 686−694.
(16) Glatter, O. *J. Appl. Crystallogr.* **1977**, *10*, 415−421.
(17) Roe, R.-J. *Methods of X-Ray and Neutron Scattering in Polymer Science*; Oxford University Press: New York, 2000.
(18) (a) Giacomelli, F. C.; Riegel, I. C.; Petzhold, C. L.; da Silveira, N. P.; Stepanek, P. *Langmuir* **2009**, *25*, 3487−3493. (b) Pedersen, J. S.; Gerstenberg, M. C. *Macromolecules* **1996**, *29*, 1363−1365. (c) Jensen, G. V.; Shi, Q.; Hernansanz, M. J.; Oliveira, C. L. P.; Deen, G. R.; Almdal, K.; Pedersen, J. S. *J. Appl. Crystallogr.* **2011**, *44*, 473−482.
(19) Rathgeber, S.; Monkenbusch, M.; Kreitschmann, M.; Urban, V.; Brulet, A. *J. Chem. Phys.* **2002**, *117*, 4047−4062.
(20) (a) Daoud, M.; Cotton, J. *J. Phys. (Paris)* **1982**, *43*, 531−538. (b) Hayter, J. B.; Penfold, J. *Colloid Polym. Sci.* **1983**, *261*, 1022−1030.
(21) (a) Orrah, D. J.; Semlyen, J. A.; Ross-Murphy, S. B. *Polymer* **1988**, *29*, 1455−1458. (b) von Meerwall, E.; Ozisik, R.; Mattice, W. L.; Pfister, P. M. *J. Chem. Phys.* **2003**, *118*, 3867−3873.